REPRODUCTION
RESEARCH

Estrogen receptor β controls MMP-19 expression in mouse ovaries during ovulation

Ivan Nalvarte[1], Virpi Töhönen[1], Maria Lindeberg[1], Mukesh Varshney[1], Jan-Åke Gustafsson[1,2] and José Inzunza[1]

[1]*Department of Biosciences and Nutrition, Karolinska Institutet, SE-14183 Huddinge, Sweden and*
[2]*Center for Nuclear Receptors and Signaling, University of Houston, Houston, Texas 77204-5056, USA*

Correspondence should be addressed to J Inzunza; Email: jose.inzunza@ki.se

Abstract

Estrogen receptor beta (ERβ/ESR2) has a central role in mouse ovaries, as ERβ knockout (BERKO) mice are subfertile due to an increase in fibrosis around the maturing follicle and a decrease in blood supply. This has a consequence that these follicles rarely rupture to release the mature oocyte. Matrix metalloproteinases (MMPs) are modulators of the extracellular matrix, and the expression of one specific MMP, MMP-19, is normally increased in granulosa cells during their maturation until ovulation. In this study, we demonstrate that MMP-19 levels are downregulated in BERKO mouse ovaries. Using human MCF-7 cells that overexpress ERβ, we could identify MMP-19 to be a transcriptional target of ligand-bound activated ERβ acting on a specificity protein-1 binding site. These data provide a molecular explanation for the observed follicle rupture defect that contributes to the subfertility of female BERKO mice.
Reproduction (2016) **151** 253–259

Introduction

Primary targets of the female sex hormone estrogen are the mammary gland and uterus in females. Additionally, estrogen is a modulator of cellular growth and differentiation in both males and females, and essential for maintenance and proper functioning of the bone, cardiovascular system, brain, prostate, breast, urogenital tract, and immune system (Gujar *et al.* 2013, Jia *et al.* 2015). Estrogen exerts several of its effects through two classical steroid nuclear hormone receptors, estrogen receptor alpha (ERα/ESR1) and estrogen receptor beta (ERβ/ESR2). Each receptor mediates very distinct functions of estrogen, which may overlap or oppose each other (Jia *et al.* 2015).

Both receptors are required for normal function of the ovary. ERα is expressed in the theca layer and ERβ in granulosa cells (Cheng *et al.* 2002, Inzunza *et al.* 2007). While ERα knockout female mice are completely infertile with hemorrhagic cystic ovaries (Couse *et al.* 2005), the female ERβ knockout (BERKO) mice are subfertile. The defect in the female BERKO mice has been localized to a late step in follicular maturation and rupture, leading to very rare ovulation in these mice (Krege *et al.* 1998, Inzunza *et al.* 2007).

Ovulation is a well-defined physiological process regulated by hormones and growth factors culminating in liberation of the mature ovum from the preovulatory follicle into the periovulatory space (Hsueh *et al.* 1984, Richards *et al.* 1987). A tightly regulated proteolytic degradation of basement membranes and the connective tissue that constitutes the follicle wall is required for successful completion of this process.

The matrix metalloproteinases (MMPs) and their tissue inhibitors of MPs (TIMPs) have been postulated to play a critical role in the extracellular matrix (ECM) remodeling associated with many physiological and pathological processes, such as embryo implantation, inflammation, cancer, follicular development, and ovulation (Alexander & Werb 1992, Khokha *et al.* 1995, Smith *et al.* 1999, Curry & Osteen 2003). The MMPs are a family of extracellular proteinases that can be classified into different subfamilies according to their primary structures, domain organization, cellular localization, and substrate specificity.

Several studies have shown increased MMP-19 expression in periovulatory follicles in mouse and rat ovaries (Hagglund *et al.* 1999, Jo & Curry 2004). This could be more strongly observed in gonadotropin-induced ovaries where MMP-19 and its inhibitor TIMP-1 revealed a different expression pattern compared to the other MMPs and TIMPs that were expressed at a constitutive level throughout the periovulatory period. Both MMP-19 and TIMP-1 mRNA were localized to the granulosa and thecal–interstitial cells of large preovulatory and ovulating follicles (Hagglund *et al.* 1999). Findings from these studies indicated important roles for MMP-19 during follicular maturation, ovulation, and

© 2016 Society for Reproduction and Fertility
ISSN 1470–1626 (paper) 1741–7899 (online)
DOI: 10.1530/REP-15-0522
Online version via www.reproduction-online.org
Downloaded from Bioscientifica.com at 03/30/2023 02:49:01PM
via free access

luteal regression and encouraged us to investigate whether MMP-19 expression is dysregulated in BERKO mice, which could contribute to the observed subfertility in these mice.

Materials and methods

Animal experiments and ethics statement

Animals used for this study were female BERKO mice and WT littermates obtained from breeding of heterozygous male and female mice. Mice were housed (12 h light:12 h darkness, at a temperature of 21–22 °C, and a relative humidity of 50–62%) in polycarbonate plastic cages (Scambur, Koge, Denmark) containing wood chips bedding with free access to fresh water and food pellets, at the sterile animal facility of Karolinska University Hospital (Huddinge, Sweden). All mice in the BERKO colony, which were originally on a C57BL/6J/129 background, were backcrossed for 11 generations with C57BL/6 mice. Mating and genotyping of WT and BERKO mice as well as the use of mature BERKO and WT female mice as oocyte donors is described earlier (Inzunza *et al.* 2007). Ovarian stimulation was performed by one i.p. administration of 5 IU pregnant mare's serum gonadotropin (PMSG, Folligon, Intervet, Sollentuna, Sweden). After 48 h, the mice were injected intra-peritoneally with the second gonadotropin injection of human chorionic gonadotropin (hCG) 5 IU (Chorulon, Intervet). The female mice were sacrificed either after 12 h by cervical dislocation, and the ovaries were dissected and stored in RNAlater medium (Ambion) at −80 °C for RNA extraction or flash frozen for protein extraction. A total of nine BERKO mice and nine WT mice were sacrificed in three separate experiments.

All animal experiments were performed in accordance with the guidelines and approval of the local ethical committee.

MCF-7 cell culture

MCF-7 human breast adenocarcinoma cells were cultured in DMEM (containing 1 mg/ml glucose) supplemented with 10% FCS (all from Life Technologies). ERβ overexpressing MCF-7 cells were generated using the tet-off system (MCF-7–ERβ), as described earlier (Papoutsi *et al.* 2009). These cells were cultured as above without 1 μg/ml tetracycline (Sigma) for at least 4 days. ERβ levels were monitored by western blot (see below). All cells were cultured at 37 °C and 5% CO_2 in a humidified incubator. When cells were treated with ERα- or ERβ-specific ligands (10 nM 4,4′,4″-(4-propyl-(1H)-pyrazole-1,3,5-triyl)trisphenol, PPT, or 10 nM 2,3-bis(4-hydroxyphenyl)-propionitrile (DPN), respectively both from Tocris, Bristol, UK), the media was changed to phenol-free DMEM (Life Technologies) supplemented with 5% dextran charcoal-(DCC) treated FCS (Thermo Scientific, Stockholm, Sweden) 3 days prior to ligand treatment (see below).

RNA extraction, RT and quantitative real-time PCR

Total RNA from MCF-7 cells or WT and BERKO ovaries was extracted using the RNeasy mini kit (Qiagen) according to the manufacturer's protocol. Elution of mRNA was performed with 50 μl RNase-free water. cDNA was synthesized from mRNA using the SuperScript III first-strand synthesis system with oligo $(dT)_{20}$ primers (Life Technologies). Quantitative real-time PCR (qPCR) measurements were performed using 1 μl cDNA, 200 nM forward and reverse primers (Supplementary Table 1, see section on supplementary data given at the end of this article), and the SYBR green PCR master mix (Applied Biosystems) according to manufacturer's instructions. qPCRs were setup and run on a 7500 fast real-time PCR system (Applied Biosystems). Each qPCR was performed in triplicates in three different runs with negative controls. Relative mRNA expression was analyzed using the $\Delta\Delta C_t$ method normalized to *Gapdh* levels. Where indicated the cells were treated with DMSO, 10 nM PPT, or 10 nM DPN for 6 h prior to RNA extraction.

Western blot analysis

The ERβ antibody was generated by immunizing rabbits with 1 mg purified ERβ–ligand-binding domain (LBD) motif (a.a. 320–527, a kind gift from Dr X Lou, Houston Methodist Hospital) divided into four immunizations. The final bleed serum was then purified using ERβ–LBD coupled to cyanogen bromide sepharose according to manufacturer's instructions (GE Healthcare). WT and BERKO ovaries were washed in ice-cold PBS and suspended in radioimmunoprecipitation assay lysis buffer (50 mM Tris–HCl, pH 8.0, 150 mM NaCl, 5 mM EDTA, 0.5% (v/v) Nonidet P-40, 0.5% (v/v) Triton X-100, 0.1% sodium deoxycholate, 1 mM Dithiothreitol (DTT), and 1× EDTA-free protease inhibitor cocktail) (Roche). The tissues were homogenized for 20 s in a FastPrep-24 homogenizer (MP Biomedicals), followed by 1 min sonication to shear the DNA. The supernatants were collected by 10 min centrifugation at 10 000 ***g***, +4 °C and stored at −80 °C until use. Similar procedures were followed for MCF-7 cells with the exception that no FastPrep-24 homogenizer was used. In total, 30 μg extracts per lane were separated using SDS–PAGE, and proteins were electrotransferred to a PVDF membrane (Bio–Rad Laboratories), blocked in TBS-T starting block solution (Thermo Scientific), and probed using rabbit anti-human ERβ–LBD antibody, rabbit anti-human ERα antibody (MC-20, Santa Cruz Biotechnology), rabbit anti-human MMP-19 antibody (Sigma–Aldrich), rabbit anti-human TIMP-1 antibody (H-150, Santa Cruz Biotechnology), and mouse anti-human β-actin antibody (Sigma–Aldrich). The bound antibodies were visualized using anti-mouse or anti-rabbit HRP-linked secondary antibody (GE Life Sciences, Uppsala, Sweden) and ECL detection kit (GE Life Sciences). Quantification was performed using the freely available ImageJ software (http://imagej.nih.gov/ij/). Where indicated the cells were treated with DMSO, 10 nM PPT, 10 nM DPN, or 10 μM of the c-Jun inhibitor SP600125 (Tocris) for 72 h prior to cell harvest.

Chromatin immunoprecipitation

Chromatin immunoprecipitation (ChIP) assays were performed as described earlier (Tammimies *et al.* 2012) with slight modifications. Briefly, MCF-7 or MCF-7–ERβ cells were grown on 15 cm inner diameter culture plates to 80–90% confluency in phenol red-free DMEM supplemented with

Downloaded from Bioscientifica.com at 03/30/2023 02:49:01PM
via free access

5% DCC-treated FCS (Thermo Scientific) for 48 h. After treating with 10 nM DPN, 10 nM PPT, or DMSO for 45 min, cells were washed with PBS, and chromatin was cross-linked for 15 min with 1.5% formaldehyde in PBS. Cells were harvested and nuclear extracts were procured. Chromatin was sonicated using a Bioruptor (Diagenode, Liege, Belgium), and a fraction of the soluble chromatin was put aside as input material. ChIP was performed overnight with 2 µg of the indicated antibodies and magnetic protein sepharose G (Life Technologies). The antibodies were rabbit anti-human ERβ–LBD (prepared in-house), rabbit anti-human ERα (MC-20), rabbit anti-human c-Jun (H-79), and normal rabbit IgG (sc-2763) (all from Santa Cruz Biotechnology). After washing, the sepharose beads were eluted three times with 50 µl elution buffer (0.1 M $NaHCO_3$, 1% SDS), and bound chromatin was reverse cross-linked overnight at 65 °C. Eluted DNA fragments were isolated and purified using QIAquick PCR purification kit (Qiagen) and analyzed by real-time qPCR normalized to input and relative to IgG (primers listed in Supplementary Table 1).

Electromobility shift assay

Nuclear extract from MCF-7–ERβ cells was prepared, as described previously (Tammimies *et al.* 2012). Electromobility shift assay (EMSA) was performed using the EMSA kit from Life Technologies following the manufacturers' instructions with some slight modifications. In brief, indicated amount of nuclear extracts were incubated with gel shift buffer (4% glycerol, 1 mM $MgCl_2$, 0.5 mM EDTA, 50 mM Tris–HCl, pH 7.5, and 0.5 mM DTT), 3 pmol annealed probe (Supplementary Table 1), and 100 nM DPN or PPT, in a total volume of 12 µl. The reaction was incubated for 30 min at 25 °C and then resolved on 6% PAGE. The nucleic acid was visualized using 1× SYBR green solution (EMSA kit, Life Technologies) on the ChemiDoc gel imaging system (Bio–Rad Laboratories). Quantification was done using the ImageJ software (NIH Software).

Statistical analysis

Unless stated otherwise, statistical significance was determined using an unpaired, two-tailed Student's *t* test, assuming unequal variances (single comparisons), or a one-way ANOVA followed by the Tukey *post hoc* test (multiple comparisons). Differences were considered significant if the *P* value was $*P<0.05$, $**P<0.01$, and $***P<0.001$ for all tests.

Results

MMP-19 levels are downregulated in BERKO mouse ovaries following hCG-induced ovulation

Previous studies show that both ERβ and MMP-19 are specifically expressed in the granulosa cells of the follicle (Hagglund *et al.* 1999, Inzunza *et al.* 2007). With these studies in mind, we set out to determine if MMP-19 levels are lower in BERKO ovaries. To this end, WT and BERKO mice were sacrificed 12 h post hCG treatment, and ovaries were removed for RNA isolation and western blot analysis. Both ERα and ERβ were present in the WT ovarian extracts; however, in BERKO ovaries, only ERα was present (Fig. 1A). Interestingly, MMP-19 mRNA (Fig. 1B) and protein (Fig. 1C) levels were significantly lower in BERKO ovaries compared to WT ovaries. The levels of the tissue inhibitor of MMP-19, TIMP-1, were also lower in BERKO ovaries, but the difference did not reach significance. Thus, our following studies focused on MMP-19.

MMP-19 levels are increased in MCF-7 cells overexpressing ERβ

We next analyzed if MMP-19 levels change in the ERα-positive MCF-7 cells generated to overexpress ERβ (MCF-7 + ERβ, Fig. 2A). ERβ overexpression alone had no significant effect on MMP-19 protein levels. However, both the ERβ-selective agonist DPN and the ERα-selective agonist PPT were able to increase MMP-19 protein (Fig. 2B) and mRNA levels (Fig. 2C) significantly, suggesting that MMP-19 is a target gene for both ERs.

Both ERα and ERβ bind to a promoter region of the MMP-19 gene

We next investigated whether MMP-19 is a direct transcriptional target of the ERs. Using the UCSC

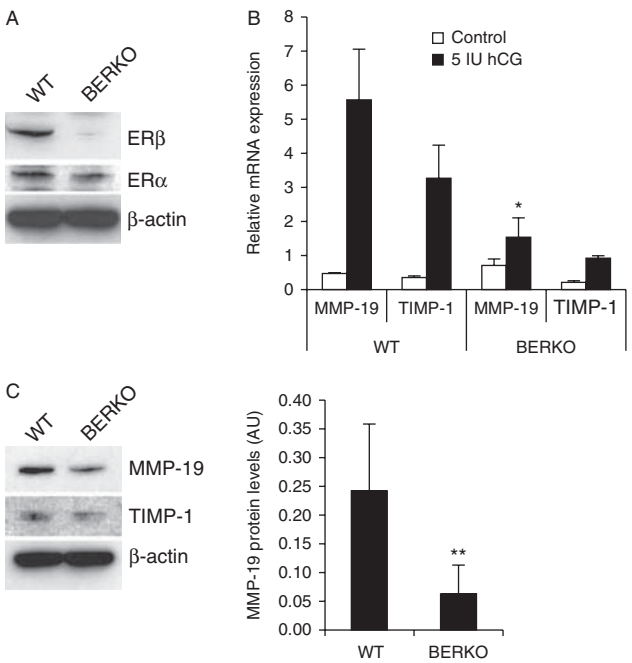

Figure 1 Expression of ER, MMP-19, and TIMP-1 in BERKO ovaries. (A) Western blot analysis of ERα and ERβ protein levels in WT and ERβ knockout (BERKO) ovaries ($n=3$). (B) MMP-19 and TIMP-1 mRNA expression in WT and BERKO ovaries after 48 h PMSG and 12 h vehicle (control) or 5 IU hCG treatment ($n=3$). (C) Western blot analysis (left panel) and quantification (right panel) of MMP-19 and TIMP-1 protein levels (normalized to β-actin levels) in ovaries from PMSG and 5 IU hCG-treated WT and BERKO mice ($n=4$). AU, arbitrary units. $*P<0.05$ and $**P<0.01$ compared to similarly treated WT mice.

Downloaded from Bioscientifica.com at 03/30/2023 02:49:01PM
via free access

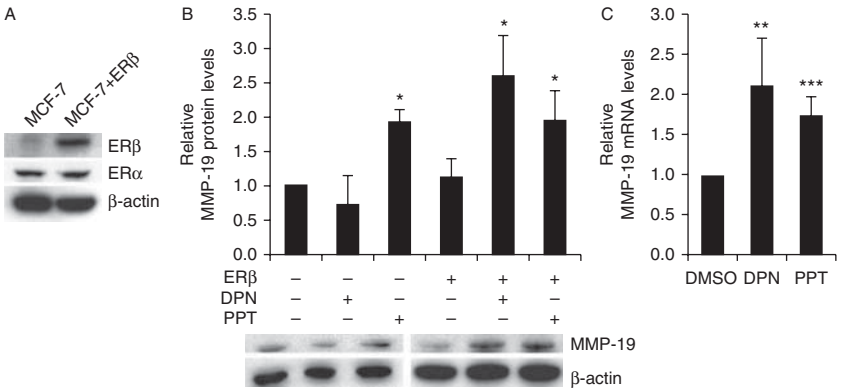

Figure 2 Expression of MMP-19 in MCF-7+ERβ cells. (A) Western blot analysis of ERα and ERβ protein levels in MCF-7 and MCF-7+ERβ cells. (B) Quantification of relative MMP-19 protein levels (normalized to β-actin levels) in MCF-7 and MCF-7+ERβ cells after 72 h stimulation with 10 nM of the indicated ligand ($n=4$). (C) MMP-19 mRNA expression after 6 h DMSO (vehicle), 10 nM DPN, or 10 nM PPT treatment ($n=8$). $^{*}P<0.05$, $^{**}P<0.01$, and $^{***}P<0.001$ compared to DMSO-treated control.

Genome Browser (v319, http://genome-euro.ucsc.edu) and the TFBIND (http://tfbind.hgc.jp, RIKEN Center for Integrative Medical Sciences) search algorithms, we could not detect any clear estrogen response elements searching 10 000 bp upstream of the transcription start site (TSS) or within the human *MMP-19* or mouse *Mmp-19* gene. However, several activating protein-1 (AP1) and specificity protein-1 (Sp1) sites were detected in the proximal promoter (Fig. 3A). ERs are known to bind to such sites tethered to either AP1 or Sp1 to mediate both ligand dependent and independent transcription (Kushner *et al.* 2000, Safe & Kim 2008). Thus, we analyzed if ERα and/or ERβ bind to one of the identified sites. Using ChIP assays, we found that ERβ was recruited to a region containing an AP1/Sp1 site upon DPN treatment in MCF-7+ERβ cells (Fig. 3B), located 1215 bases upstream of the translation start site and 1062 bases upstream of the TSS of the *MMP19* gene (AP1/Sp1 site #3). No ERβ enrichment was found in the absence of ligand or upon treatment with PPT. Furthermore, we could not find any ER enrichment at any other analyzed region (data not shown). ERα was enriched at AP1/Sp1 site #3 upon treatment with the ERα-selective agonist PPT. The AP1 complex member, c-Jun, was also enriched at this site upon PPT treatment, suggesting an interaction between ERα and AP1 here. Of note, we could also observe a ligand-independent recruitment of ERα here, which could suggest that ERα may also bind this region without ligand stimulation. On the other hand, ERβ only binds to this region in a ligand- (DPN) dependent manner and not via c-Jun but possibly through another transcriptional complex or to another recognition sequence, for example to the Sp1 site. No ER or c-Jun enrichment was found at a non-related sequence containing a serum response factor (SRF)-binding site (Fig. 3B).

This finding was further elaborated in EMSAs using a probe that encompasses the specific AP1 and Sp1 site (Fig. 3C), and corresponds to the region to which both ERα and ERβ bound in the ChIP assay. As expected, DPN treatment resulted in a clear band whose intensity was increased with increasing amounts of MCF-7+ERβ nuclear extract (Fig. 3D). This effect was not seen with PPT treatment, which resulted in formation of a complex of roughly similar size but where intensities were comparable to DMSO vehicle treatment alone, suggesting that less complexes are formed or needed to mediate the effect of PPT. The dependence on either AP1 or Sp1 site was analyzed using AP1, Sp1, or AP1–Sp1 mutated probes (Supplementary Table 1). As seen in Fig. 3E, DPN treatment increased the complex formation on the non-mutated WT probe. When the AP1 site was mutated to a sequence without a recognition site for a specific transcription factor, we could see a surprising increase in proteins bound to this probe. However, this increase was ligand independent, suggesting that non-specific factors bind this probe. In contrast, mutation of the Sp1 site abolished the DPN-mediated increase in complex formation, which was also the case when using the AP1–Sp1 mutated probe (Fig. 3E), although unspecific complexes also appeared to bind this latter probe to some extent both with and without DPN stimulation. Thus, these data point out ERβ, and not ERα, as the main isoform driving estrogen-dependent expression of MMP-19 here.

Inhibition of Sp1, but not AP1 binding, abolishes DPN-dependent MMP-19 expression

We then went on to further elucidate the roles of AP1 and Sp1 in mediating the effects of ER on MMP-19 regulation. We treated MCF-7 and MCF-7+ERβ cells with the c-Jun N-terminal kinase inhibitor SP600125 that abolishes c-Jun phosphorylation and activation, or the Sp1 family inhibitor mithramycin A (MithA). As expected, PPT treatment increased MMP-19 levels (Fig. 4). However, upon concomitant PPT and SP600125 treatment, the MMP-19 protein levels significantly dropped. This was evident in both MCF-7 and MCF-7+ERβ cells. On the other hand, MMP-19 levels remained high in DPN-treated MCF-7+ERβ cells even with SP600125 treatment (Fig. 4). Treatment of MCF-7+ERβ cells with MithA abolished the DPN-mediated increase in MMP-19 levels, but not the PPT-mediated increase (Fig. 4). These data suggest that the ERα-mediated MMP-19 expression is likely dependent on the formation of an AP1 complex, whereas the

Downloaded from Bioscientifica.com at 03/30/2023 02:49:01PM
via free access

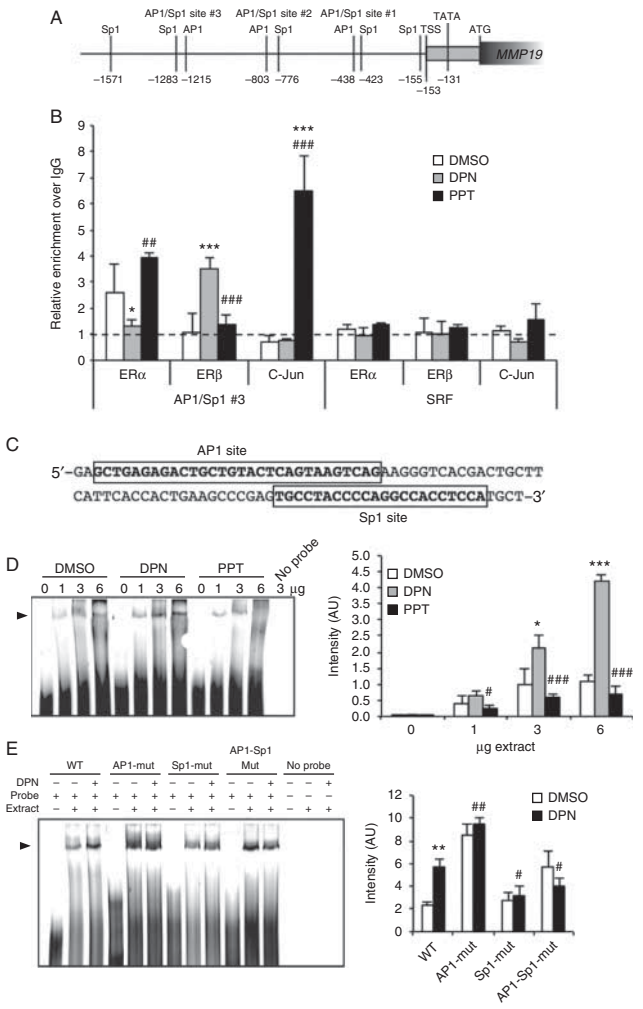

Figure 3 PPT- and DPN-dependent enrichment of ER and c-Jun complexes to MMP-19 promoter sequence. (A) Schematic illustration of analyzed AP1/Sp1 binding regions in the MMP19 proximal promoter (transcription start site (TSS); TATA, TATA-box). (B) Relative enrichment over non-specific IgG of ERα, ERβ, and c-Jun to an AP1–Sp1 site in the MMP-19 promoter or to a non-specific serum response factor (SRF) site. MCF-7+ERβ cells were treated with DMSO, 10 nM DPN, or 10 nM PPT prior to cross-linking and cell harvest ($n=4$). (C) WT nucleotide probe used for EMSA analyses (AP1/Sp1 site #3). Boxes show the AP1 and Sp1 site. (D) EMSA of indicated amounts of MCF-7+ERβ nuclear extracts binding to the WT probe upon DMSO, 100 nM DPN, or 100 nM PPT treatment. Right panel, quantification ($n=3$). (E) EMSA of DPN (100 nM) treated MCF-7+ERβ nuclear extracts (3 µg) binding to the WT or AP1, Sp1, and AP1–Sp1 mutated probes (see Supplementary Table 1). Right panel, quantification ($n=3$). AU, arbitrary units, arrowhead indicate probe-binding complexes. $^{*}P<0.05$ $^{**}P<0.01$, and $^{***}P<0.001$ compared to DMSO treatment and WT probe. $^{\#}P<0.05$, $^{\#\#}P<0.01$ and $^{\#\#\#}P<0.001$ compared to DPN treatment and WT probe.

ERβ-mediated MMP-19 expression is dependent on Sp1 family transcription factor binding.

In conclusion, we provide evidence that *MMP-19* is an ERβ target gene, where ERβ requires a specific Sp1 site on the *MMP-19* promoter to mediate ligand dependent transcription. This provides mechanistic insights into the role of ERβ in the granulosa cells of the follicle and provides an explanation to why lack of ERβ, but not ERα, results in increased fibrosis and follicular rupture defects.

Discussion

The causes for reduced fertility can be many. Female mice lacking ERβ (BERKO) are subfertile. Although the ovarian follicles grow and differentiate initially normally in these mice, the follicles rarely rupture to ovulate, and the BERKO ovaries display fewer corpora lutea (Cheng *et al.* 2002, Inzunza *et al.* 2007). Previous studies have pointed out a vascularization defect in BERKO ovaries and increased fibrosis in the thecal layers surrounding the maturing follicle (Inzunza *et al.* 2007). Interestingly, wedge resection of BERKO ovaries completely, but transiently, restored fertility supposedly through an adequate rush of blood supply, cytokines, and chemokines. Thus, the increased fibrosis in BERKO ovaries is likely the cause for the inadequate blood supply and follicle rupture defect. MMPs are key proteases that regulate deposition of collagen in the ECM of most tissues and inhibit fibrosis (Giannandrea & Parks 2014). Several MMPs exist in the ovary (MMP-2, MMP-11, MMP-14, and MMP-19) of which only MMP-19 is strongly increased in the granulosa and thecal–interstitial cells of the preovulatory and ovulating follicles (Hagglund *et al.* 1999, Jo & Curry 2004). This increase in MMP-19 expression coincides with the massive surge in preovulatory estrogen levels. Importantly, we see a downregulation of MMP-19 message and protein levels in BERKO ovaries compared to WT ovaries. This could very well explain the increase in fibrous tissue in BERKO ovaries and thus the deregulated blood supply to the follicle and its difficulties to rupture to release the ovum. Our study shows that both ERα and ERβ can regulate *MMP19* gene expression in a ligand-dependent manner by binding to a promoter sequence of *MMP19*

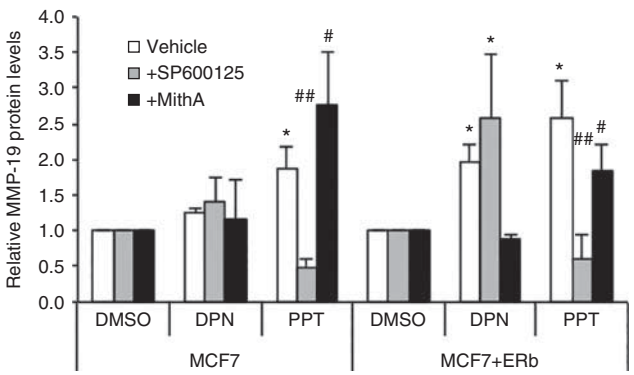

Figure 4 The DPN-mediated expression of MMP-19 is Sp1 dependent. Quantification of MMP-19 protein levels in MCF-7 and MCF-7+ERβ cells after DMSO, DPN, or PPT treatment and concomitant SP600125 or mithramycin A (MithA) treatment for 72 h ($n=3$). $^{*}P<0.05$ compared to DMSO treatment, $^{\#}P<0.05$ and $^{\#\#}P<0.01$ compared to DPN treatment.

Downloaded from Bioscientifica.com at 03/30/2023 02:49:01PM
via free access

encompassing an AP1 and Sp1 binding site. ERα is present in the thecal layer and the stroma, whereas ERβ is only present in the granulosa cells of growing and mature follicles (Couse *et al.* 2005, Inzunza *et al.* 2007). Hence, ERα could modulate the MMP-19 expression in the thecal layer and thereby prevent fibrosis. However, this appears not to be the case or is not sufficient, since ERα is still present in fibrous BERKO ovaries. Instead, our data suggest that it is ERβ that drives the MMP-19 expression in the maturing granulosa cells and that lack of this expression results in the described increase in fibrous tissue around the follicle (Inzunza *et al.* 2007), thus resulting in a rupture defect of mature follicles.

In our studies, we could observe a ligand-dependent enrichment of ERβ to an Sp1 site in the MMP-19 promoter that also encompasses an AP1 site. Sp1 sites are very common in promoter regions, and ERβ has been reported to bind tethered to Sp1 in both ligand-dependent and -independent manner (Kushner *et al.* 2000, Safe & Kim 2008). Nevertheless, direct binding to the DNA cannot be excluded here. In addition, contrary to ERα, ERβ does not appear to have a strong preference for a specific consensus sequence and has been shown to bind at distal enhancer sites and intergenic regions to a greater extent than to promoter regions (Vivar *et al.* 2010). Therefore, we also cannot exclude other binding sites of ERβ that could modulate MMP-19 expression in addition to the one identified in the present study.

In summary, we put forth the evidence that MMP-19 is an ERβ target gene in mouse ovaries and that ERβ drives its expression in a ligand-dependent fashion. These data explain our previous finding that lack of ERβ results in increased fibrosis around the follicle that results in decreased vascularization, a follicle rupture defect, and subfertility. Our data also suggest that ERβ could be a promising target in treating subfertility.

Supplementary data

This is linked to the online version of the paper at http://dx.doi.org/10.1530/REP-15-0522.

Declaration of interest

The authors declare that there is no conflict of interest that could be perceived as prejudicing the impartiality of the research reported.

Funding

This work was supported by the Center for Innovative Medicine (CIMED), the Swedish Cancer Fund (grant number CAN2013/377), and the Tore Nilson's and Magnus Bergvall's foundations (J Inzunza). The Robert A Welch Foundation (E-0004) supported J-Å Gustafsson.

Author contribution statement

I Nalvarte and V Töhönen performed the experiments analyzed data and wrote the manuscript; M Lindeberg performed experiments, analyzed data, and commented on the manuscript; M Varshney performed experiments and commented on the manuscript; J-Å Gustafsson conceived the project and commented on the manuscript; and J Inzunza conceived the project, analyzed data, and wrote the manuscript.

Acknowledgements

The authors thank Anne-Marie Witte for technical support and genotyping the BERKO mice, and Dr Joëlle Rüegg for critical evaluation of the manuscript.

References

Alexander CM & Werb Z 1992 Targeted disruption of the tissue inhibitor of metalloproteinases gene increases the invasive behavior of primitive mesenchymal cells derived from embryonic stem cells *in vitro*. *Journal of Cell Biology* **118** 727–739. (doi:10.1083/jcb.118.3.727)

Cheng G, Weihua Z, Makinen S, Makela S, Saji S, Warner M, Gustafsson JA & Hovatta O 2002 A role for the androgen receptor in follicular atresia of estrogen receptor β knockout mouse ovary. *Biology of Reproduction* **66** 77–84. (doi:10.1095/biolreprod66.1.77)

Couse JF, Yates MM, Deroo BJ & Korach KS 2005 Estrogen receptor-β is critical to granulosa cell differentiation and the ovulatory response to gonadotropins. *Endocrinology* **146** 3247–3262. (doi:10.1210/en.2005-0213)

Curry TE Jr & Osteen KG 2003 The matrix metalloproteinase system: changes, regulation, and impact throughout the ovarian and uterine reproductive cycle. *Endocrine Reviews* **24** 428–465. (doi:10.1210/er.2002-0005)

Giannandrea M & Parks WC 2014 Diverse functions of matrix metalloproteinases during fibrosis. *Disease Models & Mechanisms* **7** 193–203. (doi:10.1242/dmm.012062)

Gujar S, Dielschneider R, Clements D, Helson E, Shmulevitz M, Marcato P, Pan D, Pan LZ, Ahn DG, Alawadhi A *et al.* 2013 Multifaceted therapeutic targeting of ovarian peritoneal carcinomatosis through virus-induced immunomodulation. *Molecular Therapy* **21** 338–347. (doi:10.1038/mt.2012.228)

Hagglund AC, Ny A, Leonardsson G & Ny T 1999 Regulation and localization of matrix metalloproteinases and tissue inhibitors of metalloproteinases in the mouse ovary during gonadotropin-induced ovulation. *Endocrinology* **140** 4351–4358. (doi:10.1210/endo.140.9.7002)

Hsueh AJ, Adashi EY, Jones PB & Welsh TH Jr 1984 Hormonal regulation of the differentiation of cultured ovarian granulosa cells. *Endocrine Reviews* **5** 76–127. (doi:10.1210/edrv-5-1-76)

Inzunza J, Morani A, Cheng G, Warner M, Hreinsson J, Gustafsson JA & Hovatta O 2007 Ovarian wedge resection restores fertility in estrogen receptor beta knockout ($ER\beta^{-/-}$) mice. *PNAS* **104** 600–605. (doi:10.1073/pnas.0608951103)

Jia M, Dahlman-Wright K & Gustafsson JA 2015 Estrogen receptor alpha and beta in health and disease. *Best practice & Research Clinical Endocrinology & Metabolism* **29** 557–568. (doi:10.1016/j.beem.2015.04.008)

Jo M & Curry TE Jr 2004 Regulation of matrix metalloproteinase-19 messenger RNA expression in the rat ovary. *Biology of Reproduction* **71** 1796–1806. (doi:10.1095/biolreprod.104.031823)

Khokha R, Martin DC & Fata JE 1995 Utilization of transgenic mice in the study of matrix degrading proteinases and their inhibitors. *Cancer Metastasis Reviews* **14** 97–111. (doi:10.1007/BF00665794)

Krege JH, Hodgin JB, Couse JF, Enmark E, Warner M, Mahler JF, Sar M, Korach KS, Gustafsson JA & Smithies O 1998 Generation and reproductive phenotypes of mice lacking estrogen receptor β. *PNAS* **95** 15677–15682. (doi:10.1073/pnas.95.26.15677)

Kushner PJ, Agard DA, Greene GL, Scanlan TS, Shiau AK, Uht RM & Webb P 2000 Estrogen receptor pathways to AP-1. *Journal of Steroid Biochemistry and Molecular Biology* **74** 311–317. (doi:10.1016/S0960-0760(00)00108-4)

Downloaded from Bioscientifica.com at 03/30/2023 02:49:01PM
via free access

Papoutsi Z, Zhao C, Putnik M, Gustafsson JA & Dahlman-Wright K 2009 Binding of estrogen receptor α/β heterodimers to chromatin in MCF-7 cells. *Journal of Molecular Endocrinology* **43** 65–72. (doi:10.1677/JME-08-0177)

Richards JS, Jahnsen T, Hedin L, Lifka J, Ratoosh S, Durica JM & Goldring NB 1987 Ovarian follicular development: from physiology to molecular biology. *Recent Progress in Hormone Research* **43** 231–276.

Safe S & Kim K 2008 Non-classical genomic estrogen receptor (ER)/specificity protein and ER/activating protein-1 signaling pathways. *Journal of Molecular Endocrinology* **41** 263–275. (doi:10.1677/JME-08-0103)

Smith MF, McIntush EW, Ricke WA, Kojima FN & Smith GW 1999 Regulation of ovarian extracellular matrix remodelling by metalloproteinases and their tissue inhibitors: effects on follicular development, ovulation and luteal function. *Journal of Reproduction and Fertility. Supplement* **54** 367–381.

Tammimies K, Tapia-Paez I, Ruegg J, Rosin G, Kere J, Gustafsson JA & Nalvarte I 2012 The rs3743205 SNP is important for the regulation of the dyslexia candidate gene DYX1C1 by estrogen receptor β and DNA methylation. *Molecular Endocrinology* **26** 619–629. (doi:10.1210/me.2011-1376)

Vivar OI, Zhao X, Saunier EF, Griffin C, Mayba OS, Tagliaferri M, Cohen I, Speed TP & Leitman DC 2010 Estrogen receptor β binds to and regulates three distinct classes of target genes. *Journal of Biological Chemistry* **285** 22059–22066. (doi:10.1074/jbc.M110.114116)

Received 4 November 2015
First decision 8 December 2015
Revised manuscript received 13 December 2015
Accepted 22 December 2015

Downloaded from Bioscientifica.com at 03/30/2023 02:49:01PM
via free access